
CHAPTER - I V

MAGNETISATION STUDIES

4.1 Introduction

The nature of application of a ferrite is decided by its hysteresis studies which furnish an invaluable data on the permeability μ , the saturation magnetisation M_s , the coercive force H_c , and the remanance ratio M_r/M_s . The wide range of permeability values of ferrites make them suitable for various frequency ranges. The coercive force varies from 0.1 Oe upto 3000 Oe. Ferrites with low H_c , called soft ferrites are used in the manufacture of high frequency inductances, cores of transformers, motors and generators. The overall requirements of these applications are high permeability, low coercive force, and small hysteresis losses. Hard ferrites are the ferrites with high H_c and are generally employed as permanent magnets for various kinds of electric motors, loud speakers, telephones, TV and other appliances which also need high remanance. Neel in 1949 has shown that the coercive force H_c is related with the crystal anisotropy, the saturation magnetisation, the internal stresses and the porosity¹. The ^{Squareness} ratio determines the usefulness of the ferrites in the magnetic memory and switching devices. Hysteresis properties are highly dependent on chemical constitution and crystal structure, porosity and grain size distribution, heat treatment and machining history² and so on. The preparation of ferrites with good squareness of loop characteristics demands most stringent conditions and atmosphere.

Experimental techniques for the measurement of magnetic properties of ferrites are described by Maxwell. The saturation magnetisation forms an important basic parameter and its measurement can be made by the ballistic method, the vibration coil magnetometer, the vibrating sample magnetometer, various force methods and microwave methods. We have used high field loop tracer HS 869 supplied by Electronics Corporation of India, for the measurements on hysteresis for the samples.

A brief survey of the theory pertaining to the phenomenon of hysteresis is presented in this chapter in order to make the discussion of the results.

4.2 Domains and Wall Formation

Weiss³ in 1907 postulated the existence of molecular field responsible for the spontaneous alignment of atomic magnets. However, the fact that ferromagnetic crystals frequently exhibit the state of zero magnetisation, led to the prediction of randomly oriented domains. Barkhausen⁴ in 1919 showed that the magnetisation of the specimen changes discontinuously when the applied field changes continuously. This supported the interpretation that the magnetisation is due to rotation of magnetisations of the whole domains. Landau and Lifshitz showed that in any ferromagnetic material domain formation results as a consequence of considerable reduction in magnetostatic energy from that of the state of saturated magnetisation.

Weiss could not elucidate the origin of molecular field but stated that the interactions of magnetic moments of the electrons are too weak to explain the large molecular field. Heisenberg⁵ in 1928 gave the quantum mechanical explanation of the alignment in terms of exchange interaction between the uncompensated spins of electrons in the partially filled 3-d shells. He showed that under certain conditions the exchange energy produces effects similar to those of Weiss molecular field. In this case electrons with parallel spins have lower energy than those with antiparallel alignment. Spontaneous magnetisation can also arise as a result of negative exchange interactions under favourable conditions of intervening ions. Neel⁶ in 1948 showed that in this case, the neighbouring magnetic moments are antiparallel. This is the origin of spontaneous magnetisation in ferrites where there are magnetic moments arranged in antiparallel or some other complex fashion compensating partially. The magnetic moments contributing to the magnetisation are mainly spin magnetic moments due to the quenching of orbital angular momentum. The non-integral values of the magneton numbers in case of Fe, Ni, Co at 0°K could not be explained by the Heisenberg model but has been explained on the basis of band theory of solids (Stoner 1933)⁷. The exchange energy is given by

$$W_{\text{ex}} = 2 JS^2 \sum_{i \neq j} \cos \phi_{ij}$$

where S is the total spin momentum per atom and ϕ_{ij} is the angle between the spin momentum vectors of atoms i and j .

Here anisotropy is neglected and only nearest neighbour exchange interactions are considered. The exchange energy alone would not show the observed anisotropy in the magnetic properties of a crystal involving easy axes of magnetisation. This implies existence of an interaction between the spins and the crystal lattice. For a cubic crystal the excess energy needed to magnetise a crystal in a given direction as compared to that required for an easy direction is given by

$$W_k = K_1(\alpha_1^2\alpha_2^2 + \alpha_2^2\alpha_3^2 + \alpha_3^2\alpha_1^2) + K_2\alpha_1^2\alpha_2^2\alpha_3^2 + \dots$$

where K_1 and K_2 are the anisotropy constants characteristic of the particular material and $\alpha_1, \alpha_2, \alpha_3$ are the direction cosines of magnetisation vectors with respect to the cubic axes.

When the crystal is strained there is change in the anisotropy energy which is called the magneto-elastic energy W_λ . It is due to change in interatomic spacing. One more contribution to the energy is that of magnetostatic energy W_M , which is the work required to assemble all the dipoles constituting the body. The magnetostatic energy needs to be reduced which occurs as a result of division of crystal into domains. This subdivision halts at a point where the energy required for the formation of an additional domain wall becomes greater than the decrease in the magnetostatic energy.

Bloch⁸ in 1932 has shown that the change in the magnetisation between two neighbouring domains takes place over a finite

width. If it has to occur over a unit interatomic distance very high value of exchange energy would be required. This wall of ferrite width contains spins whose orientations gradually change from the direction in one domain to that in the other. Thus the atomic spins within the wall do not remain parallel to an easy direction and so lead to some anisotropy energy. There are two types of walls - 180° walls and 90° walls. The spins rotate by 180° from one domain to the other in the former case and by 90° in the latter case. The thickness of the domain wall is determined by the condition of minimum total energy, it is given by $\delta = \left(\frac{A}{k}\right)^{1/2}$; this leads to wall energy $W_w = 4\sqrt{AK}$; where A is the exchange energy constant and k is anisotropy constant⁹. In principle the optimum domain configuration can be determined from the condition of minimum free energy i.e. by minimising $W = W_{ex} + W_k + W_\lambda + W_M + W_r$ for particular value of applied field. The shape of the magnetisation curve for a crystal can be determined by repeating this procedure for the various values of the applied field, but in practice it is full of difficulties.

It is seen that a Bloch wall appears when there is a transition of magnetisation from a given direction to any other under the condition of zero-divergence of magnetisation across the wall.

When the thickness of the specimen is small, of the order of the width of the domain wall, the interactions between the

strips of free poles formed at the intersections of the wall with the specimen surface becomes important. This was first pointed out by Neel¹⁰ in the year 1935. He predicted a new type of transition. The wall is called a Neel wall. Here the magnetisation rotates from one domain to the neighbouring one while remaining in the plane of the film. In case of the films (thin specimens) Neel walls become energetically favoured. This work has been extended by Middlehoek¹¹ wherein the energy for different transitions is given as a function of angles between orientations of neighbouring domains.

There is one more type of spin transition in which the wall is called crossed tie wall. Here the short right angled cross-ties are regularly arranged. This structure is explained by considering the variation of the closure of flux at alternate intervals through the plane of spin rotation around the spiraling axis of the wall. Middlehoek¹² in 1963, has shown that the energy of a wall of cross-tie type is roughly 0.6 times the energy of Neel wall. From the theory it appears that Bloch wall is formed in specimens of thickness greater than approximately 900 \AA and for specimens with thickness less than about 900 \AA , cross tie wall is most favoured. According to these theoretical considerations Neel wall is not expected to be formed at all. However, in specimens of thickness less than about 200 \AA Neel walls are observed.

Experimentally more complex walls have been observed where spin rotations are complex; such walls may consist of alternate

sections of pure Bloch type of transitions and pure Neel type of transitions with regions of complex combinations of both types in between the two to achieve continuity.

For polycrystalline material with grains that are not very small the domain structures for each grain are roughly similar to those in large crystals. Of course, there will be modifications in the domain structure due to small dimensions of the grains and due to interaction between adjacent grains. Results in case of polycrystalline ferrites are similar to those as observed for single crystals.

4.3 Irreversibility and Hysteresis

Generally irreversibility and hysteresis in ferromagnetic materials are attributed to impediments to the motion of domain walls offered by defects like inclusion, heterogeneties due to other phase and dislocations¹³. Magnetisation proceeds by reversible wall motion at small fields and above threshold field by irreversible wall motion and at very high fields by irreversible rotations. Above the threshold field, Barkhausen jumps are observed in magnetisation, when the wall energy is maximum. This leads to irreversible increase in magnetostatic and magneto-elastic energies of the material under the action of external magnetic field. When the magnetic field is reduced to zero, the residual magnetisation remains locked, the thermal energy required for randomisation and wall motion not being available. Also during magnetisation reversal nucleation has to proceed

before the sequence of reversible and irreversible wall motion and spin rotation can take place. Therefore, for a unisolated specimen the changes result in hysteresis during the magnetisation cycle, signifying the energy loss. A model of wall motion proposed by Kersten¹⁴ in 1943 for an inhomogeneous material having nonmagnetic inclusion considers changes in the energy of the domain wall due to variations of the area of the wall.

The strain and the inclusion theories considered only plane domain walls and regular arrays of imperfections and also did not deal with the magnetic disturbances created by the imperfections. However, in view of the statistically distributed imperfections, the number of imperfections that will be intersected by the wall on an average would remain the same. This does not portray a variation in the wall energy leading to small coercivity. Further work on the problem led Neel to establish that there are variations in the magnitude and direction of the magnetization due to the randomly distributed irregularities within the same domain. From this dispersed field theory Neel calculated critical field required for irreversible moments of domain wall and the coercivity.

Goodenough¹⁵ in 1954 has presented in detail the nucleation centres of reverse domains in a saturated polycrystalline specimen considering the magnetostatic energy associated with the defects. He examined the effects of granular inclusions, lamellar precipitates, grain boundaries and the crystal surface and arrived at

the conclusion that these are the most likely centres of reverse domain formation. When a magnetic material consists of fine particles, likely to be single domain, the process of magnetisation reversal can only take place by rotation through the hard direction with consequent irreversibility. The studies on the coercivity of the sample having single domain particles with uniaxial anisotropy imbedded in a matrix showed that the demagnetising fields of the particles themselves determine the coercivity¹⁶. However, Stoner and Wohlfarth's calculations of coercivity do not agree with the values reached in practice. This can be partly explained by the magnetic interactions between the particles and the possibility of other mechanisms of magnetisation reversal like fanning reversal mechanism, incoherent spin rotation by magnetisation buckling and magnetisation curling¹⁷.

4.4 Losses

When a magnetic material is used in an alternating magnetic field, a certain portion of the magnetic energy is absorbed by the material and dissipated as heat. If alternating field is $H = H_0 \exp(i\omega t)$, then the induction B can, in general, be represented as

$$B = B_0 \exp i(\omega t + \delta) \quad \dots (5.1)$$

so that

$$\begin{aligned} \mu = B/H &= B_0/H_0 (\cos \delta + i \sin \delta) \\ &= \mu' + i\mu'' \end{aligned} \quad \dots (5.2)$$

where μ' gives that component of the flux which is in phase,

and μ'' the one that is 90° out of phase with the applied field. The energy loss per cycle can be shown proportional to μ'' . The ratio $\frac{\mu''}{\mu'}$ = $\tan \delta$ is called power factor or loss factor. The quality factor, 'Q' is defined as

$$Q = \frac{\mu'}{\mu''} = \frac{1}{\tan \delta} \quad \dots (5.3)$$

From the point of view of applications, the variation of μ' and μ'' against frequency is an important criterion and is called magnetic or permeability spectrum.

The important mechanisms of losses are (1) hysteresis, (2) eddy current, (3) spin resonance, (4) relaxation, and (5) wall resonance for Ferrites working at low fields the hysteresis and eddy current losses are relatively small, and the major contribution comes from the remaining sources.

4.4.1 Hysteresis Loss

The energy dE required to change magnetisation M to $M + dM$ at a field H is given by $dE = HdM$. Thus the total energy absorbed for a complete hysteresis cycle is

$$W = \oint HdM \quad \dots (4.4)$$

which is equal to the area under the hysteresis loop. Low coercivity or high permeability results in a small area under the loop and hence a small loss.

4.4.2 Eddy-current Loss

An electric current is induced in the magnetic core material by the alternating magnetic field. This causes heating and power loss. It is found that the power loss per second is proportional to f^2/ρ where f is the frequency and ρ the electrical resistivity of the core material, the constant of proportionality depending upon the geometry of the core.

4.4.3 Spin-resonance Loss

Under the influence of the internal anisotropy field H_k , the electron spin vector in a magnetic material precesses with frequency ω given by $\omega = \gamma H_k$, where γ is the gyromagnetic ratio. If the electron spin vector subjected to an external r-f magnetic field H_i in a direction perpendicular to that of H_k , then the resonance sets in, when the radio frequency matches the precessional frequency and energy is absorbed from the applied field. In case of a material with negative crystal anisotropy constant the rotational processes are important, then the resonant frequency is inversely proportional to $(\mu-1)$. Therefore, when the permeability of the material is higher the resonant frequency is lower.

4.4.4 Relaxation Loss

The loss that is exhibited at frequencies much lower than the resonance frequency needs to be accounted for. This has been attributed to several relaxation processes. The major

relaxation loss in ferrites is attributed to the electron exchange between Fe^{2+} and Fe^{3+} ions. As the magnetisation changes its direction, then Fe^{2+} and Fe^{3+} ions tend to change their position to attain the configuration that has the lower energy under the changed direction of magnetisation. The readjustment of the Fe^{3+} , Fe^{2+} position does not require movement of ions, but merely that of electrons.

This relaxation loss is frequency dependent, and is maximum when the applied frequency is close to the relaxation frequency for electron jump for a given material at a given temperature.

4.4.5 Wall Resonance Loss

In certain samples, the low frequency loss has been identified as due to domain wall resonance. If the domain wall is disturbed from its equilibrium position, a restoring force sets in, which tries to bring it back. The wall, like a stretched membrane, thus has a natural frequency of oscillation. If the frequency of the applied magnetic field matches this natural frequency, resonance absorption sets in.

4.5 Experimental

4.5.1 Apparatus

High field loop tracer HS 869 supplied by Electronic Corporation of India Limited, Hyderabad, was used for the measurements on hysteresis. It consists of an alternating

current electromagnet working on 50 Hz with the aid of which a sinusoidal field of maximum peak 3500 Oe is produced in about 9 mm air gap. The instrument operates on 230 volts 50 Hz a.c. A special balancing coil is used to detect the magnetisation of the sample placed in the air gap. The signal from the balancing coil after integration is proportional to the magnetic moment of the specimen and is fed to the vertical plates of an oscilloscope after suitable amplification. A signal proportional to the magnetic field is fed to the horizontal plates of the oscilloscope. Thus the oscilloscope displays magnetic moment versus field, that is, hysteresis loop for the sample. The vertical detection can be calibrated in terms of magnetic moment in e.m.u. and horizontal in Oe per division. The magnetic parameters are accurate to within five per cent. *The experimental set up is shown in fig. 4.4.*

4.5.2 Measurement Procedure :

The measurements on M_s were carried out directly from the C.R.O. screen, which was properly illuminated and calibrated, before introducing the sample in the balancing coil in the 'C' core space, the stray fields, stray signals, and phase mismatch were carefully got rid of with the aid of controls provided. Even after introducing the sample the set up was once again tested for the above mentioned interferences when the current in the electromagnet was zero. Then the current was gradually increased and the hysteresis loop was obtained on the C.R.O. screen. The divisions of the C.R.O. on Y-axis (magnetisation

axis) were calibrated using the ~~axis~~ the standard Ni strip, having the saturation magnetisation of 53.34 emu/gm.

For the measurement of Ms by hysteresis loop on C.R.O. screen, a digital multimeter was connected across the vertical deflection of C.R.O. and reading in milivolts was noted for every ferrite sample and also for standard Ni-sample.

4.6 Results and Discussion

In fig.(4.1) compositional variation of saturation magnetisation has been shown for the ferrites $Zn_xNi_{1-x}Fe_2O_4$ and $Zn_xNi_{0.8-x}Cu_{0.2}Fe_2O_4$. It is seen that as the content of zinc is increased the value of Ms also shows increasing trend upto 40 % content of zinc beyond which a decreasing trend is exhibited by the compositional variation of Ms. The values of Ms are minimum for $NiFe_2O_4$ and $Ni_{0.8}Cu_{0.2}Fe_2O_4$. The values of Ms are maximum for $Zn_{0.4}Ni_{0.6}Fe_2O_4$ and $Zn_{0.4}Ni_{0.4}Cu_{0.2}Fe_2O_4$. For nickel-zinc ferrite the values of Ms are found upto 80 % content of zinc, but with the addition of 0.2 copper the values of Ms are found upto 60 % content of zinc. Also the values of Ms are in general lowered with the addition of copper.

Srivastava et al.¹⁸ have calculated the Y-K angles for $Zn_xFe_{3-x}O_4$. R.G.Kulkarni et al.¹⁹ have carried out studies on magnetic ordering in Cu-Zn ferrite. They have calculated theoretical values of YK angles using the formula

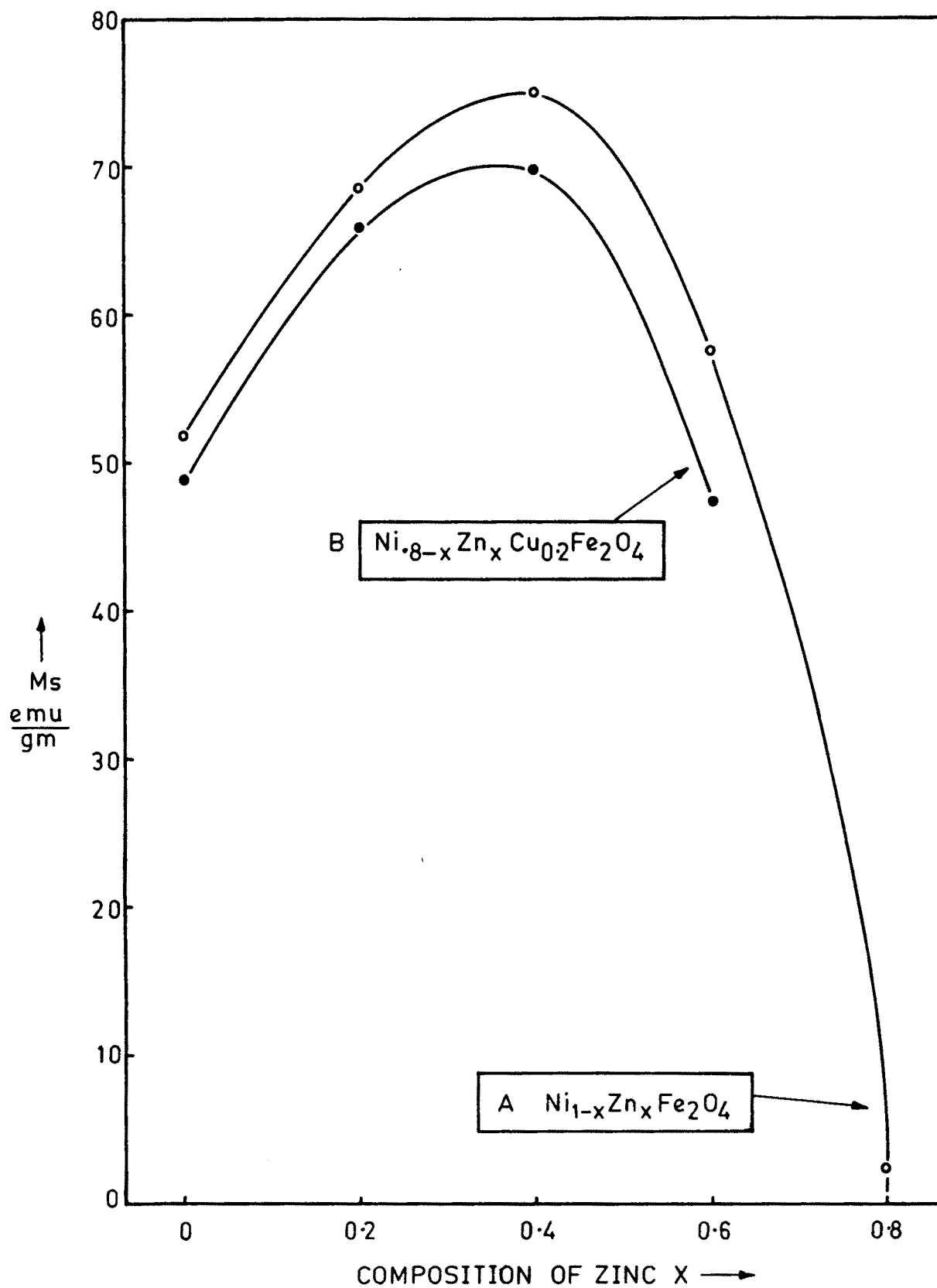


Fig.4.1 : VARIATION OF M_s vs COMPOSITION OF ZINC X .

$$\cos \alpha_{YK} = \frac{5(1-x)^2 \alpha + 25(1-x^2) \beta}{(1-x^2)\gamma + 25(1+x^2)\delta + 10(1-x^2)\epsilon}$$

They have used the values of exchange constants as follows.

$$J_{\alpha} = - 5.25, J_{\beta} = - 14.8, J_{\delta} = - 10,$$

$$J_{\gamma} = 389, J_{\epsilon} = - 4.53$$

which are calculated by Srivastava et al. They have compared the theoretical values of YK angles with those of experimental values and concluded that canted type of spins are favoured on B sub-lattice in the case of Cu-Zn ferrite. We have used the following formula for the calculation of YK angles.

$$\eta_{\beta} = (6+x) \cos \alpha_{YK} - 5 (1-x)$$

where η_{β} is expressed in the units of Bohr-magneton and x represents the content of zinc. The experimental values of magnetic moment were obtained using the formula²⁰.

$$\eta_{\beta} = \frac{\text{Mol. wt.} \times M_s}{5585 \times d_s}$$

where d_s = density of the sample, σ_s = saturation magnetisation in e.m.u. per gm.

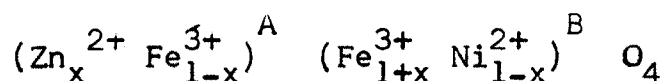
M_s was calculated as follows.

$$M_s = (1 - p) \sigma_s d_s$$

where p is the porosity.

From table(4.1) it is seen that the YK angles for NiFe_2O_4 , $\text{Zn}_{0.2}\text{Ni}_{0.8}\text{Fe}_2\text{O}_4$, $\text{Ni}_{0.8}\text{Cu}_{0.2}\text{Fe}_2\text{O}_4$ and $\text{Zn}_{0.2}\text{Ni}_{0.6}\text{Cu}_{0.2}\text{Fe}_2\text{O}_4$ are zero.

This suggests that the magnetisation variation in these ferrites can be explained on Neel two sub lattice model. For $\text{Zn}_x\text{Ni}_{1-x}\text{Fe}_2\text{O}_4$ ($x = 0, 0.2$). The cation distribution can be given as



This cation distribution is presented from the fact that Zn^{2+} is a nonmagnetic ion and has strong preference for A site²¹. On going to A site it forces equal number of Fe^{3+} ions to B site. Ni^{2+} has strong preference for B site. The net magnetic moment per formula unit is given by

$$n_\beta = [5(1+x) + m(1-x) - 5(1-x)] \text{ Bohr magneton}$$

where M is the magnetic moment of Ni^{2+} ions in Bohr magnetons.

Then it is seen that n_β has minimum value equal to M for $x=0$ for NiFe_2O_4 and which tends to 10 as the content of zinc is increased. However this value of n_β is never realised in practice. In Fig.(4.1) it is seen that the value of M_s and hence n_β goes on decreasing beyond 40 % content of zinc.

For the ferrites $\text{Zn}_x\text{Ni}_{1-x}\text{Fe}_2\text{O}_4$ and $\text{Zn}_x\text{Ni}_{0.8-x}\text{Cu}_{0.2}\text{Fe}_2\text{O}_4$ ($x > 0.2$) the Neel two sublattice model cannot be used to explain the compositional variation of M_s which is evidenced by

Table No.4.1Y-K angles for the ferrite samples

Ferrite Sample		Y-K angles
A ₁	NiFe ₂ O ₄	0°
A ₂	Ni _{0.8} Zn _{0.2} Fe ₂ O ₄	0°
A ₃	Ni _{0.6} Zn _{0.4} Fe ₂ O ₄	14° 14'
A ₄	Ni _{0.4} Zn _{0.6} Fe ₂ O ₄	46° 58'
A ₅	Ni _{0.2} Zn _{0.8} Fe ₂ O ₄	80° 36'
A ₆	ZnFe ₂ O ₄	90°

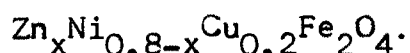
B ₁	Ni _{0.8} Cu _{0.2} Fe ₂ O ₄	0°
B ₂	Ni _{0.6} Zn _{0.2} Cu _{0.2} Fe ₂ O ₄	0°
B ₃	Ni _{0.4} Zn _{0.4} Cu _{0.2} Fe ₂ O ₄	21°
B ₄	Ni _{0.2} Zn _{0.6} Cu _{0.2} Fe ₂ O ₄	52° 10'
B ₅	Zn _{0.8} Cu _{0.2} Fe ₂ O ₄	-

the nonzero YK angles for these samples. (Table No.4.1). In both the ferrite series as the content of zinc is increased the YK angles go on increasing. Thus the change in magnetisation on zinc substitution occurs due to the presence of YK angles in the spin system on B sites. The condition for YK angles to occur in Ni-Zn system has been investigated in the molecular field approximation by Satyamurthy et al.¹⁸ using a noncolinear three sublattice model. The increase in the YK angles indicate the increasing favouring of triangular spin arrangement on B sites leading to reduction in A-B interaction. B-B interactions are antiferromagnetic even in a mixed magnetic zinc ferrite. The effect of B-B interaction is usually masked by strong A-B interaction which causes the spin on B-sites to be aligned parallel to each other. However the substitution of zinc in excess of 20 % leads to canted type of arrangements on B sites weakening the A-B interaction as suggested by Yafet and Kittel²².

When nickel in Ni-Zn ferrite is completely replaced by zinc, $\cos\alpha_{YK}$ becomes zero as $\alpha_{YK} = 90^\circ$ suggesting that B-B interaction collapses leading to a zero M_s for $ZnFe_2O_4$. Similar explanation can be applied for copper containing Ni-Zn ferrite which shows zero value of M_s .

In fig.(4.1) it is seen that with the addition of copper the values of M_s are lowered. Nickel ferrite has magnetic moment 2.3 while copper ferrite has magnetic moment 1.3²⁴. Thus the substitution of copper of lower magnetic moment in the

ferrite is expected to lower the value of M_s for



In fig.(4.2) the variation of Curie temperatures with the content of zinc in the ferrite samples $\text{Zn}_x\text{Ni}_{1-x}\text{Fe}_2\text{O}_4$ and $\text{Zn}_x\text{Ni}_{1-x}\text{Cu}_{0.2}\text{Fe}_2\text{O}_4$ is shown. It is seen that as the content of zinc in the both the ferrite systems increases the value of T_c goes on decreasing. T_c is maximum for NiFe_2O_4 and $\text{Ni}_{0.8}\text{Cu}_{0.2}\text{Fe}_2\text{O}_4$ while it is minimum for $\text{Zn}_{0.8}\text{Ni}_{0.2}\text{Fe}_2\text{O}_4$ and $\text{Zn}_{0.6}\text{Ni}_{0.2}\text{Cu}_{0.2}\text{Fe}_2\text{O}_4$. For rest of the samples the values of T_c were not observed at room temperatures.

The lowering of T_c can be well correlated with the observed values of α_{YK} angles in the ferrite. As explained previously the increase in α_{YK} angles is characterised by a decrease in A-B interaction leading to lowering of T_c in the ferrites. It is also seen from fig (4.2) that the addition of copper lowers the T_c values. This lowering can again be related with the higher magnetic moment of 2.3 for NiFe_2O_4 than 1.3 that for CuFe_2O_4 .

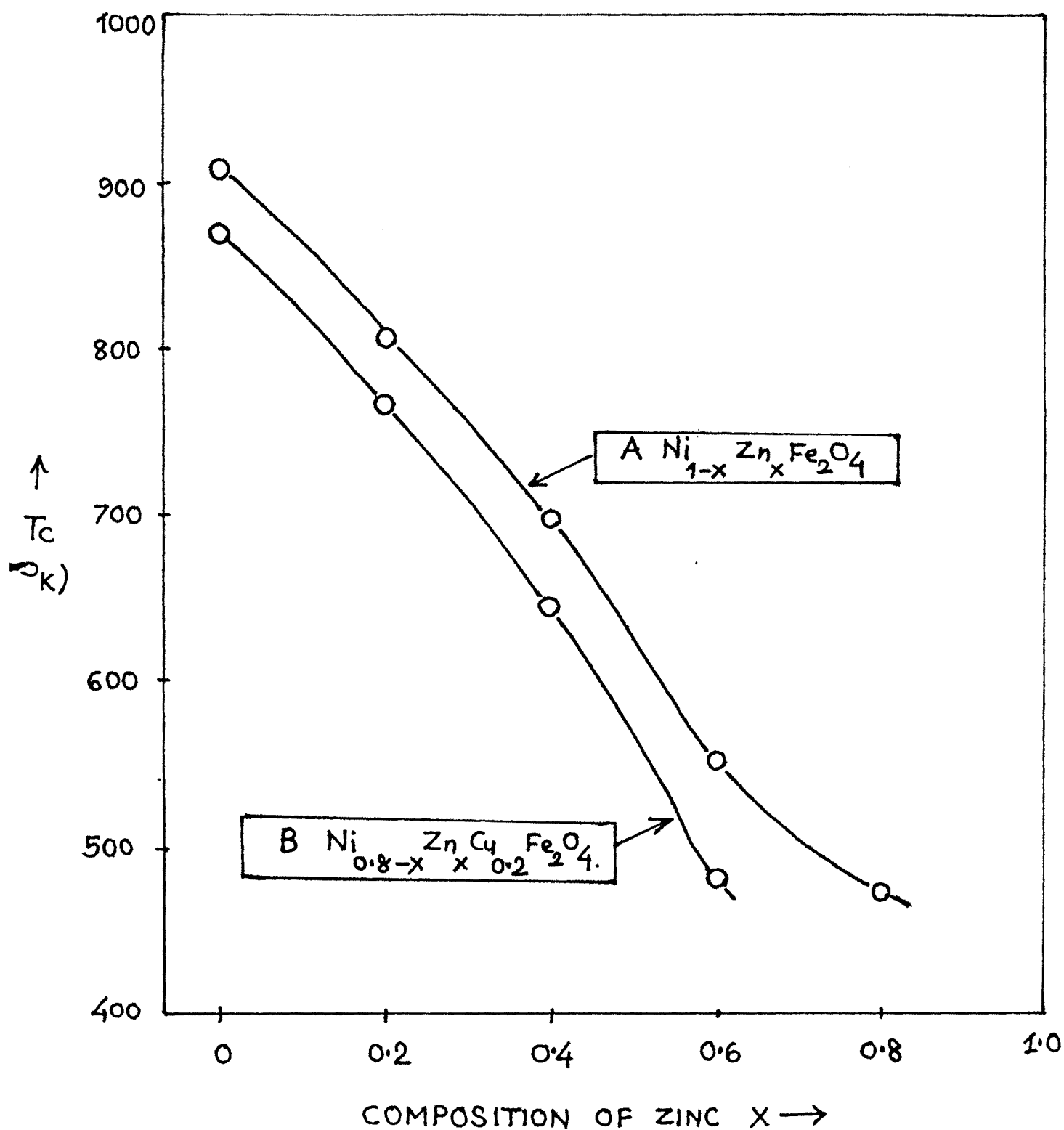


Fig. 4.2 VARIATION OF T_c vs COMPOSITION OF ZINC X

References

1. Alper, A.M., 'High temperature oxides' Academic Press N.Y. (1971).
2. Stern, E., Microwave materials and applications, Jr. Appl. Phys. Vol. 38 No. 3 (1967) p. 1397-99.
3. Weiss, P., "L hypothese du champ molecularie et la. propriete ferromagnetique" J. de Physique, 6, (1907), P. 661.
4. Barkhausen H., "Two phenomena uncovered with the help of the new amplifiers", Phys. Zeits, 20, (1919), p. 401.
5. Heisenberg W., "On the theory of ferromagnetism", Zent fur Phys, 49, (1928) p. 619.
6. Neel L., "Magnetic properties of ferrites, ferrimagnetism and antiferromagnetism", Ann Physique 3, (1948) p. 137.
7. Stoner, E.C., "Atomic moments in ferromagnetic metals and alloys with non-ferromagnetic elements", Phil. Mag., 15, (1933), p. 1018.
8. Bloch, F., "Theory of exchange problem and of residual ferromagnetism", Zeit fur Phys. 74, (1932), p. 295.
9. Sinha, A.P.B. and Menon, P.G., Solid State Chemistry, Marcel Dekker, INC, N.Y. (1974).
10. Neel, L., "Energie des puros de Bloch dans les couches minces", Compt. Rend. Acad. Sci. Paris, 241 (1955), P. 533.

11. R. Carry and E.D. Issac, Magnetic Domains and techniques for their observation, The English Univ. Press Ltd., London E.C.4 (1966).
12. Middlehoek S., "Domain walls in their Ni-Fe films", J.Appl.Phys., 34, (1963) p.1054.
13. Kondorsky E., "On the nature of the coersive force and irreversible changes in magnetisation", Physik.Z. Sowjetunion, 11, (1937) p.597.
14. Keroten, M., "Grundlagen Ciner Theorie der ferromagnetischen Hysterese und der Kuerzitivkraft, Hirzel Leipzig, (1943).
15. Goodenough J.B. "A theory of domain creation and coersive force in polycrystalline ferromagnetics, Phys.Rev.vol.95, No.4, Aug.15. (1954) p.917-932.
16. Stoner E.C. and Wohlfarth E.P., "Interpretation of high coercivity in ferromagnetic materials", Nature, 160, (1947) p.650.
17. Frei E.H., Shtrikman S. and Treves D., "Critical size and nucleation field of ideal ferromagnetic particles" Phys. Rev., 106 (1957), p.446.
18. N.S.Satyamurthy, M.G.Natera, S.I.Youssef, R.J.Begum and C.M.Srivastava, Physical Review, 181, (1969) p.969.
19. R.G.Kulkarni, Magnetic ordering in Cu-Zn ferrite, Jr. Mat.Sc., 17 (1982) p.843-848.

20. K. Sheshan, A.L. Shashimohan, D.K. Chakrabarti, A.B. Biswas, "Cation distribution and magnetic properties of Ni-MgFe₂O₄ system", N.P.S.S.P. Symposium.
21. Guillaud, Magnetic properties of ferrites, J.Phys.Rad., 12 (1951) p.239-248.
22. Y.Yafet, C.Kittel, Antiferromagnetic arrangements in Ferrites, (1952) p.290.
23. K.J. Standley, "Oxide magnetic materials", Clarendon Press, Oxford (1972) p.65.